A second wave of *Sonic hedgehog* expression during the development of the bat limb

Dorit Hockman[a], Chris J. Cretekos[b], Mandy K. Mason[c], Richard R. Behringer[d], David S. Jacobs[c], and Nicola Illing[a,1]

Departments of [a]Molecular and Cell Biology and [c]Zoology, University of Cape Town, Cape Town 7701, South Africa; [b]Department of Biological Sciences, Idaho State University, Pocatello, ID 83209; and [d]Department of Molecular Genetics, University of Texas M.D. Anderson Cancer Center, Houston, TX 77030

Edited by Brigid L. M. Hogan, Duke University Medical Center, Durham, NC, and approved September 17, 2008 (received for review May 31, 2008)

***Sonic hedgehog* (*Shh*) plays an integral role in both the anterior-posterior (A-P) patterning and expansion of developing vertebrate limbs through a feedback loop involving *Fgfs*, *Bmps*, and *Gremlin*. In bat limbs A-P patterning and the size of the digital field are unique. The posterior digits of the forelimb are elongated and joined by tissue, whereas the thumb is short. The hindlimb digits often are uniform in length. Here, we reveal novel expression patterns for *Shh* and its target, *Patched 1* (*Ptc1*), during limb development in two bat species. Early *Shh* expression in the zone of polarizing activity is wider in the bat forelimb than in the mouse forelimb, correlating with the reported expansion of *Fgf8* expression in the apical ectodermal ridge and the early loss of symmetry in the bat forelimb. Later in limb development, *Shh* and *Ptc1* expression is reinitiated in the interdigital tissue. *Shh* is graded along the A-P axis in forelimb and is expressed uniformly at a lower level across the hindlimb interdigital tissue. We also show that the reported *Fgf8* expression in the interdigital tissue precedes the expression of *Shh*. We propose that the reinitiation of *Shh* and *Fgf8* expression in bat limbs reactivates the *Shh-Fgf* feedback loop in the interdigital tissue of stage 16 bat embryos. The cell survival and proliferation signals provided by the *Shh-Fgf* signaling loop probably contribute to the lengthening of the posterior forelimb digits, the survival of the forelimb interdigital webbing, and the extension of the hindlimb digits to a uniform length.**

Miniopterus natalensis | *Carollia perspicillata* | *Patched1* | *Fgf8* | evo-devo

The hypothesis that evolutionary changes in anatomy are brought about by alterations in the regulation of key developmental "toolkit genes" is central to the field of evolutionary developmental biology. In particular, changes in the spatial and temporal regulation of the *Sonic hedgehog* (*Shh*) pathway have been implicated in the diversification of limb morphology among the vertebrates. During limb development *Shh* expression in the zone of polarizing activity (ZPA) is essential for both the growth of the digital field (1, 2, 3) and patterning of the anterior-posterior (A-P) axis of the limb bud (4). The absence of this growth signal has been implicated in the termination of hindlimb development in the dolphin (5), whereas temporal shifts in *Shh* expression lead to variations in digit number in the limbs of *Hemiergis* lizards (6).

Changes in the spatial and temporal regulation of the *Shh* pathway may be responsible for the unique skeletal structure of the bat limb, because the processes of A-P patterning and limb bud growth are dramatically altered during bat limb development. Whereas the early mouse limb buds and the bat hindlimb bud initially are symmetrical across the A-P axis, the bat forelimb autopod begins to lose this symmetry as early as stage 15 of development (CS 15), because of the expansion of the posterior autopod relative to the anterior autopod (Fig. 1*B* and *C* compared with *A*, and *F* and *G* compared with *E*) (7). Following this initial expansion, the chondrocytes in the posterior digits of the bat forelimb autopod undergo accelerated proliferation and differentiation when compared with developing digits of the bat hindlimb and the mouse (8). As a result of these developmental dynamics, digits 2 to 5 of the bat forelimb are elongated in comparison to digit 1 (thumb) (Fig. 1*L*). In contrast, the digits of the bat hindlimb are not drastically elongated, and in many bat species the hindlimb digits are identical in length (Fig. 1*X*). This limb morphology is distinct from that of the mouse, in which the forelimb and hindlimb digits 1 and 5 are shorter than the remaining digits (Fig. 1*U*). The foundation for the unique skeletal structure of the bat hindlimb is laid down at CS 16 when the most proximal anterior and posterior edges of the hindlimb autopod expand, lengthening the primordia of digits 1 and 5 (Fig. 1*R* and *S*).

In the current model for growth of the digital field in vertebrate limbs, *Shh* in the ZPA interacts with *Fgfs* in the apical ectodermal ridge (AER) through a positive feedback loop, involving the bone morphogenic protein (BMP) inhibitor, *Gremlin*, as an intermediary (reviewed in 9). This signaling loop is integral to the regulation of limb size, with cell proliferation and limb outgrowth continuing as long as it is maintained (1). Recent observations of gene-expression patterns point toward a possible alteration in the regulation of the *Shh-Fgf* positive feedback loop during bat limb development. The domain of *Fgf8* expression in the AER is significantly wider in the early (CS 14) bat embryo than in the mouse (10). Later in development (CS 16), *Fgf8* and *Gremlin* acquire novel expression domains within the interdigital mesenchyme of the bat forelimb and hindlimb autopods (11). These observations suggest that spatial and temporal changes in the activation of the *Shh-Fgf* signaling loop during bat limb development underlie the unique A-P patterning of the bat limbs and the elongation of the forelimb digits.

To test this hypothesis, we compared the spatial and temporal patterns of *Shh* expression during limb development in two species of bat, *Miniopterus natalensis* and *Carollia perspicillata*, with those in the mouse, *Mus musculus*, at morphologically matched developmental stages. We also examined the expression of *Patched1* (*Ptc1*), a downstream target of *Shh* (12), as an indicator of active *Shh* signaling. Consistent with the observed expansion of early *Fgf8* expression in the AER (10), we found that *Shh* expression in the forelimb ZPA is likewise expanded. Later in limb development, *Shh* and *Ptc1* acquire novel domains of expression within the interdigital tissue; again consistent with the observed novel expression domains of *Fgf8* and *Gremlin* (11). We show that the novel expression of *Fgf8* in the interdigital tissue precedes that of *Shh* and *Ptc1*.

Based on these findings, we propose that early enhancement of the *Shh-Fgf* feedback loop underpins the early loss of symmetry in the bat forelimb autopod. In addition, we suggest that the reinitiation of the *Shh-Fgf* feedback loop later in limb development, with different spatial dynamics in the forelimb and

Author contributions: D.H., M.K.M., D.S.J., and N.I. designed research; D.H., C.J.C., and M.K.M. performed research; C.J.C. and R.R.B. contributed new reagents/analytic tools; D.H. and N.I. analyzed data; and D.H., C.J.C., and N.I. wrote the paper.

The authors declare no conflict of interest.

This article is a PNAS Direct Submission.

Data deposition footnote: The sequences reported in this paper have been deposited in the GenBank database (accession nos. EU562193 and EU664592).

[1]To whom correspondence should be addressed. E-mail: nicola.illing@uct.ac.za.

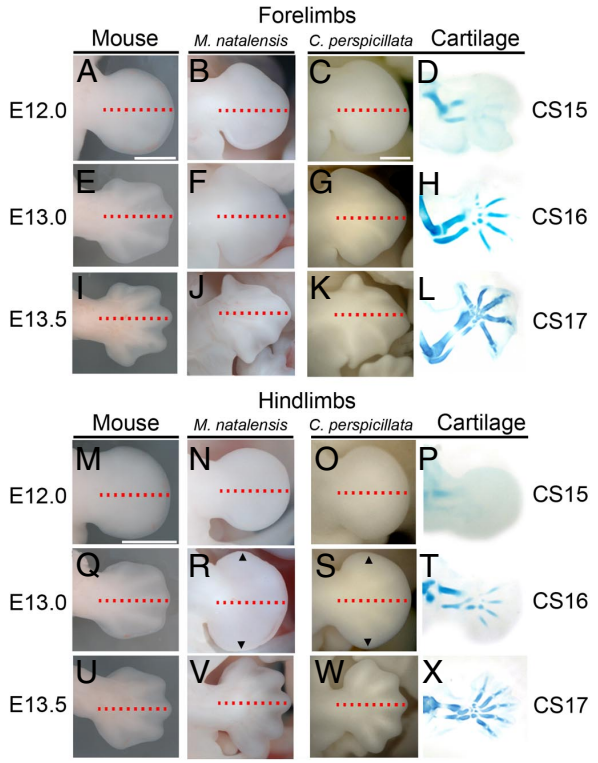

Fig. 1. Differential limb development in morphologically equivalent mouse (*M. musculus*), *M. natalensis*, and *C. perspicillata* embryos. (*A* and *M*) E12.0 mouse forelimb and hindlimb. (*E* and *Q*) E13.0 mouse forelimb and hindlimb. (*I* and *U*) E13.5 mouse forelimb and hindlimb. (*B* and *N*) CS 15 *M. natalensis* forelimb and hindlimb. (*F* and *R*) CS 16 *M. natalensis* forelimb and hindlimb. (*J* and *V*) CS 17 *M. natalensis* forelimb and hindlimb. (*C* and *O*) CS 15 *C. perspicillata* forelimb and hindlimb. (*G* and *S*) CS 16 *C. perspicillata* forelimb and hindlimb. (*K* and *W*) CS 17 *C. perspicillata* forelimb and hindlimb. (*D*, *H*, *L*, *P*, *T*, and *X*) Alcian blue staining (cartilage) of *C. perspicillata* forelimb and hindlimb at CS 15, CS 16, and CS 17. The mouse forelimbs and bat hindlimbs are symmetrical across the A-P axis, whereas the bat forelimbs begin to lose symmetry across this axis at CS 15 and more obviously at CS 16 and CS 17 because of the expansion of the posterior autopod. As a result, the posterior digits of the bat forelimb are elongated when compared with those of the mouse and the bat hindlimb. The proximal anterior and posterior edges of the bat hindlimbs are expanded at CS 16 when compared with the CS 15 hindlimbs and E13.0 mouse hindlimbs, lengthening the primordia of digits 1 and 5 by CS 17. The red dashed line indicates the plane of symmetry of the A-P axis. Arrowheads in *R* and *S* indicate the region of proximal expansion in *M. natalensis* and *C. perspicillata* hindlimbs. Anterior is up in all images. Scale bars show 0.5 mm for mouse forelimb (*A*) and hindlimb (*M*) and bat forelimb and hindlimb (*C*). *D*, *H*, *L*, *P*, *T*, and *X* are not to scale.

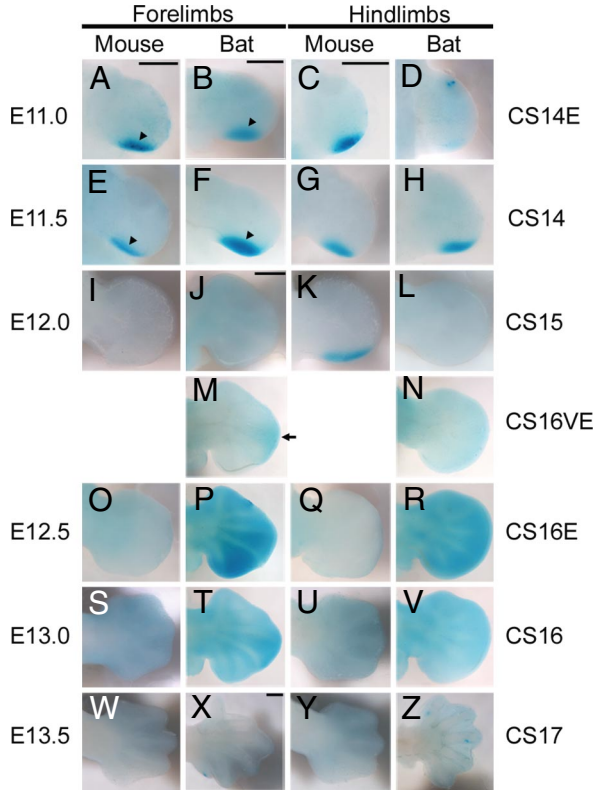

Fig. 2. *Shh* expression in morphologically equivalent mouse (*M. musculus*) and bat (*M. natalensis*) forelimbs and hindlimbs. (*A*, *E*, *I*, *O*, *S*, and *W*) Mouse forelimbs. (*C*, *G*, *K*, *Q*, *U*, and *Y*) Mouse hindlimbs. (*B*, *F*, J, *M*, *P*, *T*, and *X*) *M. natalensis* forelimbs. (*D*, *H*, L, *N*, *R*, *V*, and *Z*) *M. natalensis* hindlimbs. The embryonic (E) day of mouse development is indicated down the left side. The stage of *M. natalensis* development (CS) is indicated down the right side. Anterior is up in all images. Arrowheads in *A*, *B*, *E*, and *F* indicate the most anterior boundary of *Shh* expression in the ZPA. The arrow in *M* indicates the reinitiation of *Shh* expression in the interdigital space between digits 3 and 4. Scale bars show 0.5 mm. The scale bar in *A* also applies to *E*, *H*, *I*, and *K*. The scale bar in *C* also applies to *D* and *G*. The scale bar in *B* also applies to *F*, *L*, *N*, *O*, *Q*–*S*, *U*, and *V*. The scale bar in *J* also applies to *M*, *P*, *T*, *W*, *Y*, and *Z*.

hindlimb, contributes to the elongation of the posterior forelimb digits, the retention of the webbing between these digits, and the uniform length of all of the digits in the hindlimb.

Results

The Initiation of *Shh* Expression in the ZPA Is Delayed and the Domain of Expression Is Expanded in the Developing Bat Limb. *Shh* expression in both *M. natalensis* and mouse limbs is detected first in a posteriorly restricted domain corresponding to cells of the ZPA (Fig. 2 *A*–*H*). *Shh* is readily detectable from E10.0 (data not shown) to E11.5 in the mouse forelimb and hindlimb (Fig. 2*A*, *C*, *E*, and *G*). The corresponding *Ptc1* expression pattern is clearly graded from posterior to anterior in response to the SHH morphogenic gradient across the A-P axis (Fig. 3*A*, *C*, *E*, and *G*). The initiation of *Shh* expression seems to be delayed in the *M. natalensis* limbs. *Shh* expression in the forelimb is apparent only at CS 13L, corresponding to approximately E10.5 of mouse development (data not shown), and at a further stage later in the hindlimb (CS 14E) (Fig. 2*D*). The appearance of a corresponding graded *Ptc1* expression pattern in the *M. natalensis* limbs also is delayed by an additional stage to CS 14E in the forelimb (Fig. 3*B*) and CS 14 in the hindlimb (Fig. 3*H*).

Following the delay in *Shh* signal initiation, the domain of *Shh* expression is wider in the *M. natalensis* forelimb at CS 14E and CS 14 than in the mouse at E11.0 and E11.5 (Fig. 2*A*, *B*, *E*, and *F*; *arrowheads*). In the mouse the area of *Shh* expression hugs the posterior edge of the limb bud, whereas in *M. natalensis* the corresponding region of expression is expanded toward the centre of the limb bud. This expansion in the *Shh* expression domain at CS 14 mirrors the reported expansion in the *Fgf8* expression domain at the same stage in the AER (10) and occurs just before the initial posterior expansion of the forelimb autopod (Fig. 1*B*). In contrast, the region of *Shh* expression is not expanded in the *M. natalensis* hindlimb when compared with the mouse hindlimb (Fig. 2*G* and *H*).

Shh Expression Is Reinitiated in the Interdigital Tissue of the Developing Bat Limb. *Shh* expression in the ZPA ceases in the mouse forelimb and hindlimb by E12.0 and E12.5, respectively (Fig. 2*I* and *Q*). *Shh* also is absent from *M. natalensis* limbs by CS 15 (Fig. 2*J* and *L*). Surprisingly, during CS 16 *Shh* expression is reiniti-

DEVELOPMENTAL BIOLOGY

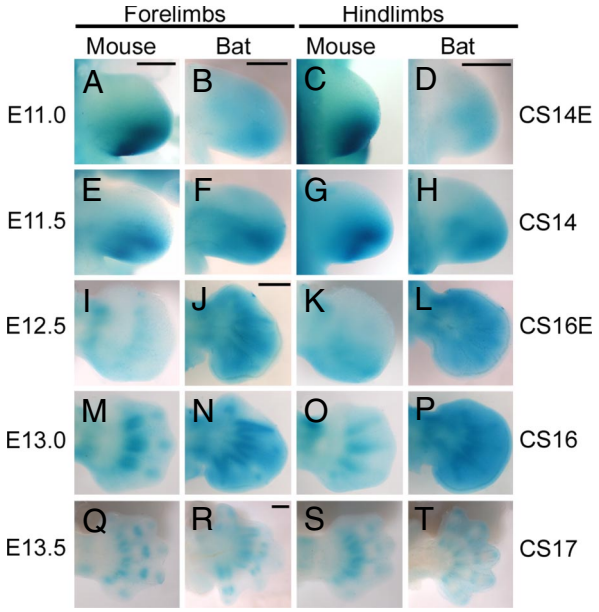

Fig. 3. *Ptc1* expression in morphologically equivalent mouse (*M. musculus*) and bat (*M. natalensis*) forelimbs and hindlimbs. (*A*, *E*, *I*, *M*, and *Q*) Mouse forelimbs. (*C*, *G*, *K*, *O*, and *S*) Mouse hindlimbs. (*B*, *F*, J, *N*, and *R*) *M. natalensis* forelimbs. (*D*, *H*, *L*, *P*, and *T*) *M. natalensis* hindlimbs. The embryonic (E) day of mouse development is indicated down the left side. The stage of *M. natalensis* development (CS) is indicated down the right side. Anterior is up in all images. Scale bars show 0.5 mm. The scale bar in *A* also applies to *C*, *E–G*, *I*, *K–M*, and *O*. The scale bar in *B* also applies to *H*. The scale bar in *J* also applies to *L*, *N*, *P*, *Q*, *S*, and T.

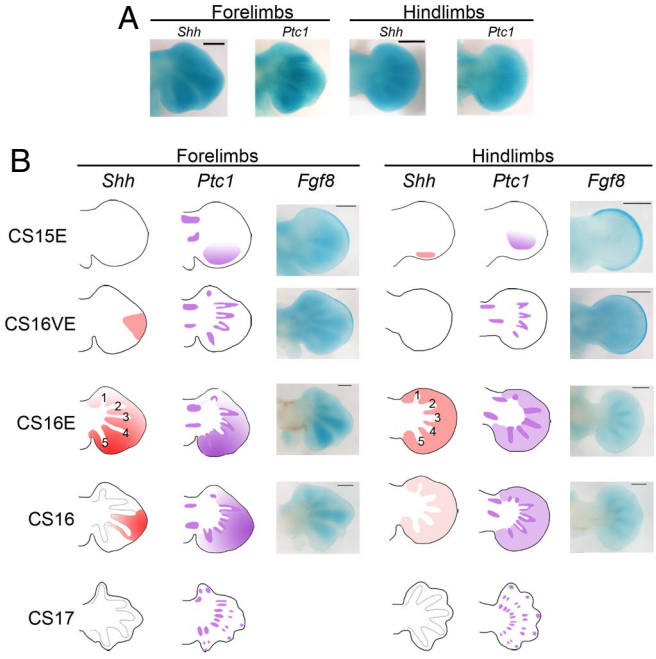

Fig. 4. (*A*) *Shh* and *Ptc1* expression in CS 16 *C. perspicillata* forelimbs (*A* and *B*) and hindlimbs (*C* and *D*). Anterior is up in all images. Both *Shh* and *Ptc1* are expressed in the interdigital tissue of both the forelimbs and the hindlimbs. Scale bars show 0.5 mm. (*B*) Summary of *Shh* and *Ptc1* expression in the forelimb and hindlimb of *M. natalensis* from CS 15E to CS 17, alongside equivalently staged *C. perspicillata* forelimbs and hindlimbs showing *Fgf8* expression. Novel *Fgf8* expression in the forelimb interdigital tissue is present before the expression of *Shh* and also is present in the forelimb and hindlimb AER at CS 15E. At this stage *Shh* (*red*) is present only at a low level in the hindlimb ZPA. At CS 16VE, novel *Fgf8* expression becomes visible in the footplate mesenchyme, in addition to the AER and interdigital tissue of the forelimb. At this stage, *Shh* expression is reinitiated at a low level in the tissue between digits 3 and 4 in the forelimb but is absent from the hindlimb. At CS 16E *Shh* in the forelimb expands to the remaining interdigital spaces and is expressed in a gradient from posterior to anterior, mirroring the *Fgf8* expression pattern. In the hindlimb, *Shh* is expressed uniformly throughout the interdigital tissue at high and low levels at CS 16E and CS 16, respectively, but *Fgf8* becomes confined to the tissue just adjacent to the digits. In the forelimb *Shh* recedes to the interdigital space between digits 3 and 4 at CS 16, but *Fgf8* persists throughout the forelimb interdigital tissue. At CS 17, *Shh* is absent from both the forelimb and hindlimb. At CS 15E *Ptc1* is expressed in a gradient from posterior to anterior in both the forelimb and hindlimb. From CS 16E to CS 17, *Ptc1* (*purple*) in the interdigital tissue corresponds to *Shh* in this domain. *Ptc1* also is expressed in the perichondrium (*dark purple*) of the developing bones, most likely in response to *Indian hedgehog*. Numbers 1 to 5 indicate digit condensations.

ated in both the forelimb and hindlimb of *M. natalensis* (Fig. 2*M*, *P*, *R*, *T*, and *V*) and *C. perspicillata* (Fig. 4 *A*). *Shh* is not detected in mouse limbs of comparable stage (Fig. 2*O*, *Q*, *S*, *U*, *W*, and *Y*). This novel expression domain is detected first in the forelimb of *M. natalensis* at very early stage 16 (CS 16VE) and is confined to the most distal region in the tissue between digits 3 and 4 (Fig. 2*M*; *arrow*). At CS 16E *Shh* expression is graded from posterior to anterior across the interdigital tissue of the forelimb, with the highest expression between digits 4 and 5 (Fig. 2*P*). *Shh* expression is reinitiated in the *M. natalensis* hindlimb during this stage and also is localized to the interdigital tissue; however, this signal is uniform along the A-P axis and is not as strong as the forelimb expression (Fig. 2*R*). Interdigital *Shh* expression persists, although at lower levels, to CS 16. At this stage, forelimb expression is highest in the tissue between digits 3 and 4 and along the borders of the condensations of all of the digits (Fig. 2*T*), whereas expression is uniformly low across the hindlimb interdigital tissue (Fig. 2*V*). By CS 17 *Shh* expression is absent from both the forelimb and hindlimb (Fig. 2*X* and *Z*).

From CS 16E to 16, *Ptc1* expression is visible in the interdigital tissue of *M. natalensis* in response to the novel *Shh* expression (Fig. 3*J*, *L*, *N*, and *P*), and similar expression is visible in *C. perspicillata* limbs at CS 16 (Fig. 4*A*). *Ptc1* is absent from this region in equivalently staged mouse limbs (Fig. 3*I*, *K*, *M*, and *O*). In both *M. natalensis* and mouse limbs, high levels of *Ptc1* expression are visible in the perichondrium of the developing digits, most likely in direct response to *Indian hedgehog* in the developing cartilage condensations (Fig. 3*I–T*) (13). This latter *Ptc1* expression is noticeably longer along the proximal-distal axis of the developing digits in the *M. natalensis* forelimb than in the *M. natalensis* hindlimb or in equivalently staged mouse limbs (Fig. 3 *M–P*), providing evidence that the primordia of the *M. natalensis* forelimb digits are longer than those of the hindlimb or the digits of the mouse limbs. In addition, the *Ptc1* expression pattern in the CS 17 *M. natalensis* hindlimb gives evidence of the symmetry of the hindlimb digits. The pattern of *Ptc1* expression is identical in each of the *M. natalensis* digit primordia, which all are of equal length (Fig. 3*T*). In the mouse hindlimb, on the other hand, the pattern of *Ptc1* expression in the short digits 1 and 5 is noticeably different from that in the longer digits (Fig. 3*S*).

Novel *Fgf8* Expression in the Interdigital Tissue of the Bat Forelimb and Hindlimb Precedes Expression of *Shh* and *Ptc1*. *Fgf8* has been shown to be expressed in a novel domain in the interdigital tissue of developing bat limbs at CS 16 and CS 17 (11). To determine whether novel *Shh* or *Fgf8* expression appears first in the interdigital tissue of developing bat limbs, we examined *Shh* and *Fgf8* expression in the contralateral limbs of bisected embryos. *Fgf8* expression becomes visible in the forelimb interdigital tissue as early as CS 15E, when *Shh* expression is absent (Fig. 4*B* and

data not shown). At this stage, *Fgf8* expression is absent from the hindlimb interdigital tissue but is present in the both the hindlimb and forelimb AER (Fig. 4*B*). From CS 16VE to CS 17, *Fgf8* expression is maintained in the forelimb interdigital tissue and is graded from posterior to anterior (Fig. 4*B*) (11). *Fgf8* becomes visible in the hindlimb mesenchyme at CS 16VE, before the appearance of the equivalent *Shh* expression (Fig. 4*B* and data not shown). *Fgf8* expression in the hindlimb becomes confined to the tissue between the digits at CS 16E (Fig. 4*B*) and is absent from the interdigital tissue by CS 17 (11). The novel interdigital expression of Fgf8 was observed in both *C. perspicillata* (Fig. 4*B*) and *M. natalensis* (data not shown).

Discussion

Early in limb development, *Shh* in the ZPA interacts in a positive feedback loop with *Fgfs* in the AER to ensure the outgrowth of the limb bud (14, 15). Here, together with data from Cretekos *et al.* (10), we provide preliminary evidence to suggest that this early signaling loop has been enhanced in the bat forelimb, leading to an expansion in the *Shh* and *Fgf8* expression domains at CS 14 of bat development. A similar phenomenon has been described in the limb buds of *Bmp* mutant mice, which display expanded *Fgf8* expression in the AER resulting from a lack of antagonism from BMPs (16). These mice also exhibit an expanded *Shh* expression domain and display posteriorly expanded limb buds. This phenotype is explained in terms of an enhanced *Shh-Fgf* interaction (16). A similar enhancement occurring naturally during bat limb development may result in a relative increase in cell proliferation and cell survival in the posterior as compared with the anterior autopod. This enhancement of the early *Shh-Fgf* signalling loop may explain the posterior expansion and resulting loss of symmetry across the A-P axis in the bat forelimb autopod at CS 15 when compared with the bat hindlimb or mouse E12.0 forelimb.

The observed expansion of the *Shh* signal in the early bat forelimb may be triggered by an autoregulatory mechanism linked to *Shh* signaling. In the developing chick limb, *Shh* has been shown to buffer its own expression, with more cells being induced to produce *Shh* if a loss of signal is induced by removing ZPA cells or by inhibiting the *Shh* signaling pathway (17, 18). The initial delay in *Shh* expression in the bat forelimb may induce this buffering mechanism, stimulating a subsequent expansion of the population of *Shh*-producing cells at CS 14E and CS 14 when compared with equivalently staged mouse limbs. Further research involving real-time analysis of *Shh* expression levels during early bat limb development compared with expression levels in the mouse may confirm this hypothesis.

At CS 16 of bat development, *Shh* and *Ptc1* are recruited to new domains of expression within the interdigital tissue of the forelimb and hindlimb (summarized in Fig. 4*B*). Interestingly, *Gremlin* and *Fgf8* also are expressed in novel domains in the interdigital tissue of *C. perspicillata* limbs at CS 16 and CS 17 (11). The observed up-regulation of all four of these genes in the interdigital tissue suggests that the *Shh-Fgf* feedback loop is initiated for a second time during bat limb development (summarized in Fig. 5). Early in limb development, *Fgf8* expression in the AER precedes the formation of the ZPA and is required to initiate and maintain *Shh* expression (15, 19). It is likely that the same is true for the interdigital expression of these genes during bat limb development. *Fgf8* is first detected in the bat forelimb and hindlimb interdigital tissue at CS 15E and CS 16VE, respectively, preceding the reinitiation of *Shh* expression at CS 16VE and CS 16E.

In the mouse and chick, the *Shh-Fgf* signaling loop involves the activation of *Gremlin* in the limb mesenchyme by SHH from the ZPA (20, 21). The *Shh*-expressing cells themselves, however, are not able to turn on *Gremlin* (22, 23). The complementary expression domains of these genes in the stage 16E forelimb

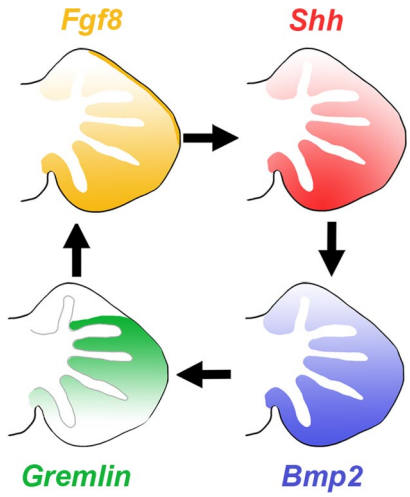

Fig. 5. A model for the reinitiation of the *Shh-Fgf* feedback loop in the interdigital tissue of the CS 16E bat forelimb. *Fgf8* (*gold*) is expressed in a novel domain within interdigital tissue of the CS 15E forelimb in a gradient from posterior to anterior as well as being expressed in the AER. We speculate that *Fgf8* activates a second wave of *Shh* (*red*) expression in the interdigital tissue at CS 16VE. *Shh* then activates of *Bmp2* (*blue*) expression in a corresponding fashion. *Bmp2* activates *Gremlin* (*green*) in a complementary domain (graded from anterior to posterior), with the highest expression located in the tissue between digits 2 and 3. *Gremlin* acts to suppress *Bmps* in the interdigital tissue, maintaining *Fgf8* expression in the interdigital tissue. *Fgf8* expression then feeds back to promote *Shh* expression in the interdigital tissue. *Bmp* and *Gremlin* expression patterns are based on stage 16 embryos (11).

suggest that the same is true when these genes are up-regulated for the second time during bat limb development. *Shh*, which is highest in the tissue between digits 3 to 5, may activate *Gremlin* in the tissue between digits 1 to 3 (11).

Bmp2 is suggested to be the link between *Shh* and *Gremlin* expression in the *Shh-Fgf* feedback loop, activating the expression of its own antagonist (23). In developing *C. perspicillata* limbs *Bmp2* expression is detected in regions corresponding to *Shh* in this study (11). Thus, it is possible that in the bat forelimb between CS 16 and CS 17, *Shh* activates *Bmp2*, which in turn activates *Gremlin* expression (Fig. 5).

Gremlin promotes *Fgf* expression in the AER, through the suppression of BMPs (20, 21). *Fgf8* in the AER then activates *Shh* expression in the ZPA, completing the *Shh-Fgf* feedback loop (15). In the CS 16 bat forelimb, *Shh* and *Fgf8* (11) are both expressed at high levels in the posterior interdigital tissue (i.e., outside the ZPA and AER, respectively) (Fig. 5). Thus, this reinitiation of the *Shh-Fgf* feedback loop differs from the earlier signaling loop in that *Shh* and *Fgf8* are able to promote each other's expression in the same domain rather than being confined to the ZPA and AER, respectively.

It is possible that the cell-proliferation and survival signals provided by the *Shh-Fgf* signaling loop are co-opted to perform the novel dual functions of lengthening the posterior forelimb digits and promoting the survival of the interdigital tissue. This model is supported by studies in the chick. These studies found that the application of SHH to the interdigital tissue of developing limbs after *Shh* expression in the ZPA has ceased prolongs *Fgf8* expression in the AER and facilitates the lengthening of the last phalange of the digits or the formation of an additional phalange and the survival of the interdigital tissue (17, 24). The extended *Fgf8* signal is described as an anti-differentiation signal, promoting the proliferation of the mesenchyme cells in the digital rays while inhibiting their differentiation into cartilage (25). *Shh* also has been shown to promote cell survival and proliferation, because a loss of *Shh* signal during limb develop-

ment results in an increase in the proportion of cells in G1 phase and a decreased proportion of cells entering S phase (26). The widespread elongation effect evident in the metacarpals and phalanges of the posterior digits of the bat forelimb may be caused by the activation of *Fgf8* and *Shh* throughout the posterior interdigital digit tissue rather than just in the AER and ZPA, respectively, exposing the metacarpals and each phalanx to the *Fgf8* and *Shh* proliferation signals.

The lack of extra phalanges in the bat forelimb digits could result from the high levels of *Shh* surrounding the digits. Retroviral-induced misexpression of *Shh* at high concentrations within the digital rays of chicken limbs blocks the formation of joints (27). In addition, *Shh* misexpression in the chondrocytes of developing mouse digits under the control of a procollagen gene promoter blocks joint formation and promotes cell proliferation (28). Thus, the high *Shh* concentration surrounding the forelimb digits in the bat may have the same effect, allowing the cells of the digital rays to proliferate and suppressing the joint-formation pathway until after *Shh* expression ceases.

Although the *Shh* and *Fgf8* signals are recruited to the interdigital tissue of the hindlimb, the duration of expression is shorter and the level is lower than in the forelimb (Fig. 4*B*) (11). In addition, the *Shh* and *Ptc1* signals are expressed uniformly across the hindlimb interdigital tissue, rather than in a gradient, as in the forelimb (Fig. 4*B*). It is possible that the short exposure to the cell-survival and proliferation signals of the *Shh-Fgf* feedback loop lengthens the primordia of digits 1 and 5 of the hindlimb but is insufficient to lengthen the remaining digits extensively or to suppress the apoptosis of the interdigital tissue. Thus, despite the early asymmetrical expression of *Shh* in the hindlimb ZPA, the late symmetrical expression of *Shh* across the hindlimb bud may contribute to the proximal expansion of the hindlimb autopod at CS 16 (Fig. 1*R*) and the growth of digits 1 and 5 to the same length as the remaining digits.

The analysis of *Shh*, *Ptc1*, and *Fgf8* expression in both *M. natalensis* and *C. perspicillata* has revealed that the novel expression domains of these genes are common within the chiropteran suborder Verspertilioniformes (29, 30). This observation suggests that the mode of wing development is constant within this taxon and supports the monophyly of the group (30, 31). Given the recent fossil find that suggests flight evolved only once in the Chiroptera (32), the mode of wing development may be common for the entire chiropteran order. If so, subtle differences in the spatial extent and timing of *Shh* expression in the forelimbs of different bat species may allow variation in the lengthening of the digits and lead to differences in adult wing shape. The analysis of *Shh* and *Ptc1* expression in the developing limbs of a species with a wing shape very different from that of *M. natalensis* and *C. perspicillata*, such as the long, narrow wings of the mollosid bats, may provide further support for this hypothesis. Analysis of the expression patterns of these genes in a species from the Pteropodiformes, the second chiropteran suborder, will reveal whether the mechanism of wing development is constant within the Chiroptera. A positive finding would provide additional support for the hypothesis that wings evolved once within this order.

It is possible that an ancient change in the highly conserved *Shh* limb-specific *cis*-regulatory region, known as the ZPA regulatory sequence (9), led to the altered *Shh* expression reported here. If indeed wings evolved once within the Chiroptera, this sequence change should be conserved across diverse bat species.

Methods

Collection and Staging of Embryos. *M. natalensis* embryos were collected from wild-caught, pregnant females in September 2006 from De Hoop Nature Reserve, Western Cape Province, South Africa (Western Cape Nature Conservation Board permit number: AAA004–00030–0035; University of Cape Town Faculty of Science Animal Experimentation Committee application number: 2006/V4/DJ). *C. perspicillata* embryos were collected from wild-caught, pregnant females on the island of Trinidad in either January or May of 2003 to 2007, as previously described (7, 8, 10, 11). The samples were collected and exported with the permission of the Wildlife Section, Forestry Division of the Ministry of Agriculture, Land and Marine Resources of the Republic of Trinidad and Tobago. All bat embryos were staged according to (7). Some of the embryos were placed in early- or late-stage categories (e.g., CS 16VE: very early; CS 16E: early; CS 16L: late) based on the progression of limb development. Mouse embryos (ICR strain) were obtained from timed matings conducted by the Animal Unit at the University of Cape Town Medical School (Animal Ethics Committee application number: 006/040).

Skeletal Imaging. The developing skeleton of bat limbs was imaged using whole-mount alcian blue staining of cartilage. *C. perspicillata* embryos at the appropriate stages were fixed overnight in Bouin's fixative (Polysciences) at room temperature, washed several times in 70% ethanol, and stained with alcian blue 8GX (Sigma) as described previously (33). After clearing in a 1:2 ratio of benzyl alcohol:benzyl benzoate, limbs were dissected, mounted in glass depression slides, and imaged under a stereodissecting Leica (model MZ9) microscope equipped with digital capture.

Gene-Expression Analysis. Whole-mount *in situ* hybridization was performed using digoxigenin-labeled RNA probes based on mouse and bat sequences. *Ptc1* primers (5′-ACCTTTGGACTGCTTCTGGGAA-3′ and 5′-AAAIGGCAAAACCTGAGT TG-3′) were designed from regions of near identity in cDNA sequence alignments of the human, mouse, rat, and dog gene and were used to clone a region of 830 bp from exon 5 to 10 of *Ptc1* from *M. natalensis* (CS 13L) and mouse (E13.5) cDNA. The *M. natalensis Ptc1* sequence has been submitted to GenBank (accession no. EU562193).

The cloned *Ptc1* sequences were used as templates in *in vitro* transcription reactions for the synthesis of bat- and mouse-specific RNA probes. A mouse *Shh* RNA probe provided by A. McMahon was used for expression analysis in both bat and mouse embryos. The sequence of this mouse *Shh* probe has been submitted to GenBank (accession no. EU664592). The *Fgf8* RNA probe used is based on the *C. perspicillata* cDNA sequence and has been described previously (10). RNA probes were used at concentration of 0.5–1 μg/ml. For analysis of dual *Shh* and *Ptc1* expression in all *M. natalensis* embryos and in E13.0 and E13.5 mouse embryos, specimens were cut in half along the midline to allow analysis of *Shh* expression on one side and *Ptc1* expression on the other. For E11.0 to E12.5 mouse embryos and for CS 16 *C. perspicillata* embryos, separate specimens were used for analysis of *Shh* and *Ptc1* expression. For analysis of dual *Shh* and *Fgf8* expression, all *M. natalensis* and *C. perspicillata* embryos were cut in half along the midline to allow analysis of *Shh* expression on one side and *Fgf8* expression on the other. One to four samples were used for each stage of development.

ACKNOWLEDGMENTS. We thank Robyn Verrinder for assistance in collecting bats and embryos at De Hoop Nature Reserve; John Rasweiler, Scott Weatherbee, and Simeon Williams for assistance in sample collection on Trinidad; the management of De Hoop Nature Reserve and the Department of Life Sciences, University of the West Indies, Trinidad for generous assistance and the use of research facilities; the Western Cape Nature Conservation Board and the Wildlife Section, Forestry Division, Agriculture Land and Marine Resources of the Republic of Trinidad and Tobago for providing collecting and export permits. Research completed in South Africa was supported by funding from a University of Cape Town Stimulation Grant and National Research Foundation Grant No 65525 (to D.S.J.). D.H. and M.K.M. were supported by National Research Foundation Prestigious Masters Scholarships. D.H. was supported by the Society for Integrative and Comparative Biology Grant-in-Aid-of-Research Award. R.R.B was supported by National Science Foundation Grant IBN 0220458. C.J.C. was supported by National Institutes of Health Training Grants CA09299 and HD07325.

1. Scherz PJ, Harfe BD, McMahon AP, Tabin CJ (2004) The limb bud *Shh-Fgf* feedback loop is terminated by expansion of former ZPA cells. *Science* 305:396–399.
2. Towers M, Mahood R, Yin Y, Tickle C (2008) Integration of growth and specification in chick wing digit-patterning. *Nature* 452:882–886.
3. Zhu J, *et al.* (2008) Uncoupling Sonic hedgehog control of pattern and expansion of the developing limb bud. *Dev Cell* 14:624–632.
4. Riddle RD, Johnson RL, Laufer E, Tabin CJ (1993) Sonic hedgehog mediates the polarizing activity of the ZPA. *Cell* 75:1401–1416.
5. Thewissen JGM, *et al.* (2006) Developmental basis for hind-limb loss in dolphins and origin of the cetacean bodyplan. *Proc Natl Acad Sci USA* 103:8414–8418.
6. Shapiro MD, Hanken J, Rosenthal N (2003) Developmental basis of evolutionary digit loss in the Australian lizard *Hemiergis*. *J Exp Zool B Mol Dev Evol* 297:48–56.

7. Cretekos CJ, *et al.* (2005) Embryonic staging system for the short-tailed fruit bat, *Carollia perspicillata*, a model organism for the Mammalian Order *Chiroptera*, based upon timed pregnancies in captive-bred animals *Dev Dyn* 233:721–738.
8. Sears KE, Behringer R, Rasweiler JJ, Niswander LA (2006) Development of bat flight: Morphologic and molecular evolution of bat wing digits. *Proc Natl Acad Sci USA* 103:6581–6586.
9. Zeller R, Zuniga A (2007) *Shh* and *Gremlin1* chromosomal landscapes in development and disease. *Curr Opin Genet Dev* 17:428–434.
10. Cretekos CJ, *et al.* (2007) Isolation, genomic structure and developmental expression of *Fgf8* in the short-tailed fruit bat, *Carollia perspicillata. Int J Dev Biol* 51:333–338.
11. Weatherbee SD, Behringer RR, Rasweiler JJ, Niswander LA (2006) Interdigital webbing retention in bat wings illustrates genetic changes underlying amniote limb diversification. *Proc Natl Acad Sci USA* 103:15103–15107.
12. Marigo V, Scott MP, Johnson RL, Goodrich LV, Tabin CJ (1996) Conservation in *hedgehog* signaling: Induction of a chicken *patched* homologue by *Sonic hedgehog* in the developing limb. *Development* 122:1225–1233.
13. Platt KA, Michaud J, Joyner AL (1997) Expression of the mouse *Gli* and *Ptc* genes is adjacent to embryonic sources of hedgehog signals suggesting a conservation of pathways between flies and mouse. *Mech Dev* 62:121–135.
14. Niswander L, Jeffry S, Martin GR, Tickle C (1994) A positive feedback loop coordinates growth and patterning in the vertebrate limb. *Nature* 371:609–612.
15. Vogel R, Rodriguez C, Izpisua-Belmonte JC (1996) Involvement of FGF-8 in initiation, outgrowth and patterning of the vertebrate limb. *Development* 122:1737–1750.
16. Bandyopadhyay A, *et al.* (2006) Genetic analysis of the roles of BMP2, BMP4, and BMP7 in limb patterning and skeletogenesis. *PloS Genet* 2:2116–2130.
17. Sanz-Ezquerro JJ, Tickle C (2000) Autoregulation of *Shh* expression and Shh induction of cell death suggest a mechanism for modulating polarising activity during chick limb development. *Development* 127:4811–4823.
18. Scherz PJ, McGlinn E, Nissim S, Tabin CJ (2007) Extended exposure to Sonic hedgehog is required for patterning the posterior digits of the vertebrate limb. *Dev Biol* 308:343–354.
19. Crossley PH, Minowada G, MacArthur CA, Martin GR (1996) Roles for FGF8 in the induction, initiation and maintenance of chick limb development. *Cell* 84:127–136.
20. Zuniga A, Haramis APG, McMahon AP, Zeller R (1999) Signal relay by BMP antagonism controls the SHH/FGF4 feedback loop in vertebrate limb buds. *Nature* 401:598–602.
21. Capdevila J, Tsukui T, Esteban CR, Zappavigna V, Belmonte JCI (1999) Control of vertebrate limb outgrowth by the proximal factor *Meis2* and distal antagonism of BMPs by Gremlin. *Mol Cell* 4:839–849.
22. Scherz PJ, Harfe BD, McMahon AP, Tabin CJ (2004) The limb bud *Shh-Fgf* feedback loop is terminated by expansion of former ZPA cells. *Science* 305:396–399.
23. Nissim S, Hasso SM, Fallon JF, Tabin CJ (2006) Regulation of *Gremlin* expression in the posterior limb bud. *Dev Biol* 299:12–21.
24. Sanz-Ezquerro JJ, Tickle C (2003) *Fgf* signaling controls the number of phalanges and tip formation in developing digits. *Curr Biol* 13:1830–1836.
25. Cassanova JC, Sanz-Ezquerro JJ (2007) Digit morphogenesis: Is the tip different? *Dev Growth Differ* 49:479–491.
26. Zhu J, *et al.* (2008) Uncoupling Sonic hedgehog control of patterning and expansion of the developing limb bud. *Developmental Cell* 14:624–632.
27. Merino R, *et al.* (1999) Expression and function of *Gdf-5* during digit skeletogenesis in the embryonic chick leg bud. *Dev Biol* 206:33–45.
28. Tavella S, *et al.* (2006) Forced chondrocyte expression of Sonic hedgehog impairs joint formation affecting proliferation and apoptosis. *Matrix Biology* 25:389–397.
29. Hutcheon JM, Kirsch JAW (2004) Camping in a different tree: Results of molecular systematic studies of bats using DNA-DNA hybridization. *Journal of Mammalian Evolution* 11:17–47.
30. Eick GN, Jacobs DS, Matthee CA (2005) A nuclear DNA phylogenetic perspective on the evolution of echolocation and historical biogeography of extant bats (Chiroptera). *Mol Biol Evol* 22:1869–1886.
31. Teeling EC, *et al.* (2005) A molecular phylogeny for bats illuminates biogeography and the fossil record. *Science* 307:580–584.
32. Simmons NB, Seymour KL, Habersetzer J, Gunnell GF (2007) Primitive early Eocene bat from Wyoming and the evolution of flight and echolocation. *Nature* 451:818–822.
33. Nagy A, Gertsenstein M, Vintersten K, Behringer R (2003) *Manipulating the Mouse Embryo*: *A Laboratory Manual* (Cold Spring Harbor Laboratory Press, New York), pp 629–706.